Proceedings of the XVII ECSMGE-2019
Geotechnical Engineering foundation of the future
ISBN 978-9935-9436-1-3

doi: 10.32075/17ECSMGE-2019-0384

XVII European Conference
ECSMGE 2019
Reykjavik
on Soil Mechanics
and Geotechnical Engineering

Comparison between energy and stress based pore pressure methods in liquefiable deposits

Comparaison entre methods d'energy et de contraintes pour la prévision de la pression interstitielle dans dépôts liquéfiables

S. Rios, M. Millen, D. Seculin, A. Viana da Fonseca
CONSTRUCT-GEO, Faculdade de Engenharia da Universidade do Porto (FEUP), Porto, Portugal

ABSTRACT: In order to mitigate the damaged induced by liquefaction events, it is imperative to evaluate the liquefaction susceptibility. Liquefaction susceptibility can either be evaluated through the retrival and testing of intact soil samples, or through procedures based on in-situ tests. Both of these frameworks are based on equivalent stress cycles (or stress-based methods), however, other types of methods (strain based or energy based) were developed with different base principles but with the same objective of predicting liquefaction triggering. In this paper the updated version of the stress based method will be compared with a dissipated energy based method, discussing their main advantages and limitations. For that purpose, nonlinear dynamic effective stress analysis were performed using the commercial software FLAC® using PM4Sand as the selected constitutive model. Using a database of 500 numerical analysis, the liquefaction triggering obtained in both simplified methods was compared with liquefaction triggering obtained in the numerical analysis. The results show that the simplified methods tend to overpredict liquefaction in comparison with the numerical analysis.

RÉSUMÉ: Les effets dévastateurs de la liquéfaction sont reconnus depuis longtemps. Afin d'atténuer les dommages induits par les événements de liquéfaction, il est impératif d'évaluer la susceptibilité à la liquéfaction. La susceptibilité à la liquéfaction peut être évaluée soit en recopiant et en testant des échantillons de sol intact, soit en utilisant des procédures basées sur des essais in situ. Ces deux methods reposent sur des cycles de contraintes équivalents (ou méthodes basées sur les contraintes). Cependant, d'autres types de méthodes (basées sur la deformation ou sur l'énergie) ont été développés avec des principes de base différents, mais avec le même objectif de prédire le déclenchement de la liquéfaction. Dans cet article, la version actuelle de la méthode basée sur les contraintes sera comparée à une méthode basée sur l'énergie, examinant leurs principaux avantages et limitations. À cette fin, une analyse dynamique non linéaire des contraintes effectives a été réalisée à l'aide du logiciel commercial FLAC® avec le PM4sand comme le modèle constitutif sélectionné. En utilisant une base de données de 500 analyses numériques, le déclenchement de la liquéfaction obtenu dans les deux méthodes simplifiées a été comparé au résultats obtenus dans l'analyse numérique. Les résultats montrent que les méthodes simplifiées ont tendance à surestimer la liquéfaction par rapport à l'analyse numérique.

Keywords: liquefaction, energy based method, numerical analysis, FLAC®, PM4sand

1 INTRODUCTION

Earthquake-induced liquefaction can cause significant damages to buildings as seen by recent events in Christchurch (Bray, Markham, et al., 2017). Although important technical achievements in liquefaction phenomena understanding and mitigation techniques have been accomplished in the last decades in the field of earthquake geotechnical engineering,

significant damage still occurs in seismic areas around the world. There are different methods in the literature to predict liquefaction triggering, these can be divided in three main groups: stress based, strain based and energy based.

One of the first methods was the well known stress based method from Seed et al., (1975) developed from cyclic triaxial tests, as a function of the normalized number of cycles to liquefaction. This method was further improved with time, the most recent adaption was described in detail by Boulanger & Idriss, (2016). The method is based on comparing the resistance of the soil in terms of the cyclic resistance ratio (CRR), with the earthquake induced cyclic stress ratio (CSR). CSR is a function of earthquake magnitude, peak surface acceleration, total and effective overburden stresses, and depth from surface. The CRR can be evaluated by different methods based on laboratory tests (e.g., cyclic triaxial tests or direct simple shear) or in situ tests (e.g., SPT, CPTU). However, the simplified stress procedure needs the conversion from PGA and magnitude to an equivalent number of cycles which is dependent on the soil properties and the ground motion properties.

A strain based method was proposed by Dobry et al., (1985) from triaxial and simple shear tests, assuming that the residual pore pressure is a function of the accumulated shear strain. Ivšić (2006) also proposed a strain based method using the damage concept introduced by Finn & Bhatia, (1982), which was then transformed into a stress based method by using the cyclic stress ratio (CSR) to define the damage parameter. This method was later improved by Park et al. (2015) and more recently by Chiaradonna et al. (2018).

The development of an energy-based liquefaction triggering method was first proposed by Davis & Berril (1982) following the assumption made by Nemat-Nasser & Shokooh, (1979) that the amount of dissipated seismic energy per unit volume of soil is uniquely correlated to the pore pressure buildup. The total amount of energy from the seismic waves arriving at a site is estimated from the total radiated energy of the earthquake and the hypocentral distance. The total radiated energy is related to the earthquake magnitude via the Gutenberg and Richter relationship. A simple energy attenuation model for spherically expanding waves that takes into account the attenuation along a ray path and geometric spreading is an inverse relationship to distance of the centre of energy release squared. The dissipated energy density is a function of the standard penetration value from SPT and the initial effective overburden stress. This method described by Davis and Berrill (1982) assumes excess pore pressure noted as to be a linear function of the dissipated energy density. However, it does not account for the radiation pattern or directivity effects associated with the individual earthquakes.

A more recent energy based triggering method was proposed by Kokusho (2013) relying on the same assumption that the pore pressure is related to the dissipated energy. Using cyclic triaxial tests, a relationship between dissipated energy and CSR (from SPT blow counts) was proposed which allowed for the method to be used as a liquefaction triggering procedure. Also based on cyclic triaxial tests, an empirical model was proposed relating the dissipated energy and strain energy, different from the common hysteretic damping ratio definition, that the author argues it does not properly reflects the energy dissipation mechanism in a sand. From the strain energy, the strain capacity of the soil is computed by multiplying the strain energy by the thickness of the layer which is compared to the upward energy. The energy ratios of individual layers are numbered sequentially starting from the lowest ratio and summed up. According to Kokusho (2013) liquefacton occurs in that sequence and in those layers for which the sum is lower than 1, because the upward energy can liquefy individual sand layers in the mentioned sequence until it is totally used by the energy capacities.

In this work, two different models were selected for comparison. The first is the stress based method (SBM) from Boulanger & Idriss,

(2016) due to its large use. The second is the energy based method (EBM) from Kokusho (2013) since it is a very complete method. Numerical analysis were performed to serve as a reference for that comparison, so that a proper identification of the advantages and limitations of the methods could be made.

2 NUMERICAL ANALYSIS DESCRIPTION

2.1 Column model

Nonlinear dynamic effective stress analysis was performed using the commercial software FLAC®.The selected constitutive model was PM4Sand (Boulanger & Ziotopoulou, 2015), a sand plasticity model developed for liquefying soils. A database of one-dimensional nonlinear effective stress analyses of 500 soil profiles was used for further understanding the behaviour of a liquefiable deposit. All models consisted of three soil layers: two non liquefiable layers made of hard clay located at the top and at the bottom while the middle layer, was made of sand. The water table was assumed at the interface of the first and second layers. In the numerical analysis the input upward propagating motion was used at the bottom of the model.

The thicknesses of the profile layers, and the soil parameters are randomly generated within a given range of values as indicated in Table 1, Equations 1, 2 and 3:

$$K = (2 * G_0 * (1 + \nu))/(3 * (1 - 2 * \nu)) \quad (1)$$

$$G_0 = 167\sqrt{(N_1)_{60} + 2.5} * P_a\sqrt{\frac{p'}{P_a}}[0.7 - 1.5] \quad (2)$$

being P_a=101300 Pa

$$h_{po} = \frac{CSR*(2.39-(2.8*D_r))}{1-CSR*(12.4-(12.9*D_r))} \quad (3)$$

The procedure to obtain CSR in equation (3) starts from the $(N_1)_{60}$ value from Table 1, and is used to calculate the CRR using the equation proposed by Idriss & Boulanger (2010), to which variability is added.

In addition, a total of 49 different ground motions selected from the NGAWest 2 database (Ancheta et al., 2013) were used (Table 2) and applied randomly to each soil profile.

Table 1. Soil parameters for the numerical analysis

Parameter	Range
General Properties	
Height of Ll, H_1	[0.5 —8.5] m
Height of L2, H_2	[0.5 —10] m
Total profile height	[20-max(2.5 • (H_1+H_2),30)] m
Permeability of Ll	$8{\cdot}10^{-8}$ m/s
Permeability of L2	$1.6{\cdot}10^{-8}$ m/s
Permeability of L3	10^{-9} m/s
Dilatancy, ψ	0º
Bulk modulus, K	Equation 1
Properties of layer 2	
Specific gravity, G_S	2.65
Poisson ratio, υ_2	0.3
Angle of shearing resistance, ϕ'	33º
Minimum void ratio, e_{min}	0.5
Maximum void ratio, e_{max}	0.8
Relative density, D_r	[0.3-0.8]
Normalised SPT, $(N_1)_{60}$	$46 \cdot Dr^2$
Norm. shear modulus, G_0 [Pa]	Equation 2
PM4Sand *hpo* factor	Equation 3
Properties of layers 1 and 3	
Maximum shear modulus, *Gi*	c' ·1000
Poisson ratio, υ_1	0.4
Specific gravity, G_S	2.7
Angle of shearing resistance, ϕ'	0º
Cohesion of L1, c'_1	[30 — 34] kPa
Cohesion of L3, c'_3	[180—200] kPa
Void ratio of Ll	[0.6 —0.8]
Void ratio of L3	[0.5 — 0.7]

Table 2. Selected input ground motions

ID	Record	E. dist [km]	Mw	Vs30 [m/s]	PGA [g]	E. kin [m^2/s^2]	Earthquake	Year	Station
1	148	9.6	5.74	350	0.26	0.27	Coyote Lake	1979	Gilroy Array #3
2	159	2.6	6.53	242	0.32	0.69	Imperial Valley-06	1979	Agrarias
3	175	32.0	6.53	197	0.14	0.44	Imperial Valley-06	1979	El Centro Array #12
4	240	2.8	5.7	382	0.55	0.20	Mammoth Lakes-04	1980	Convict Creek
5	313	19.9	6.6	361	0.35	0.46	Corinth, Greece	1981	Corinth
6	449	43.6	6.19	289	0.14	0.08	Morgan Hill	1984	Capitola
7	457	38.2	6.19	350	0.26	0.13	Morgan Hill	1984	Gilroy Array #3
8	461	3.9	6.19	282	0.32	0.42	Morgan Hill	1984	Halls Valley
9	558	14.3	6.19	316	0.42	1.06	Chalfant Valley-02	1986	Zack Brothers Ranch
10	592	9.9	5.99	368	0.31	0.22	Whittier Narrows-01	1987	Arcadia - Campus Dr
11	626	21.3	5.99	301	0.40	0.21	Whittier Narrows-01	1987	LA - 116th St School
12	692	11.7	5.99	339	0.43	0.46	Whittier Narrows-01	1987	Santa Fe Springs - E.Joslin
13	767	31.4	6.93	350	0.55	0.69	Loma Prieta	1989	Gilroy Array #3
14	770	39.9	6.93	334	0.32	0.28	Loma Prieta	1989	Gilroy Array #7
15	802	27.2	6.93	381	0.48	0.96	Loma Prieta	1989	Saratoga - Aloha Ave
16	803	27.1	6.93	348	0.42	1.45	Loma Prieta	1989	Saratoga - W Valley Coll.
17	838	94.8	7.28	370	0.14	0.35	Landers	1992	Barstow
18	848	82.1	7.28	353	0.38	1.13	Landers	1992	Coolwater
19	960	26.5	6.69	326	0.48	1.03	Northridge-01	1994	Canyon Country - W Lost Cany
20	1035	38.7	6.69	352	0.17	0.12	Northridge-01	1994	Manhattan Beach - Manhattan
21	1082	12.4	6.69	321	0.37	0.85	Northridge-01	1994	Sun Valley - Roscoe Blvd
22	1115	42.1	6.9	256	0.15	0.52	Kobe, Japan	1995	Sakai
23	1155	95.0	7.51	290	0.10	0.41	Kocaeli, Turkey	1999	Bursa Tofas
24	1158	98.2	7.51	282	0.40	1.43	Kocaeli, Turkey	1999	Duzce
25	1513	7.6	7.62	364	0.59	2.95	Chi-Chi, Taiwan	1999	TCU079
26	1605	1.6	7.14	282	0.48	2.84	Duzce, Turkey	1999	Duzce
27	2007	54.6	5.31	196	0.14	0.02	CA/Baja Border Area	2002	El Centro Array #11
28	3636	68.2	6.32	315	0.19	0.32	Taiwan SMART1(40)	1986	SMART1 I04
29	3643	69.2	6.32	307	0.22	0.20	Taiwan SMART1(40)	1986	SMART1 M02
30	3653	70.0	6.32	285	0.20	0.19	Taiwan SMART1(40)	1986	SMART1 O02
31	4066	15.1	6	227	0.55	0.21	Parkfield-02, CA	2004	PARKFIELD - FROELICH
32	4146	12.2	6	342	0.38	0.39	Parkfield-02, CA	2004	PARKFIELD - UPSAR 10
33	4159	42.3	6.63	306	0.19	0.13	Niigata, Japan	2004	FKS028
34	4169	42.5	6.63	365	0.35	0.32	Niigata, Japan	2004	FKSH21
35	4210	13.6	6.63	332	0.64	1.29	Niigata, Japan	2004	NIG020
36	4212	30.1	6.63	193	0.33	0.28	Niigata, Japan	2004	NIG022
37	4866	8.5	6.8	338	0.35	0.76	Chuetsu-oki	2007	Kawanishi Izumozaki
38	4889	58.1	6.8	315	0.37	0.37	Chuetsu-oki	2007	Joetsu Otemachi
39	5263	22.6	6.8	274	0.26	0.46	Chuetsu-oki	2007	NIG017
40	5495	39.2	6.9	288	0.25	0.45	Iwate	2008	AKTH19
41	5616	88.6	6.9	364	0.20	0.09	Iwate	2008	IWT007
42	5664	32.1	6.9	361	0.43	5.13	Iwate	2008	MYG005
43	5669	75.3	6.9	275	0.11	0.17	Iwate	2008	MYG010
44	5814	51.2	6.9	248	0.34	2.21	Iwate	2008	Furukawa Osaki City
45	5827	18.8	7.2	242	0.54	3.35	El Mayor-Cucapah	2010	MICHOACAN DE OCAMPO
46	5829	32.4	7.2	242	0.41	2.67	El Mayor-Cucapah	2010	RIITO
47	5836	55.3	7.2	265	0.45	1.46	El Mayor-Cucapah	2010	El Centro - Meloland Geot. Array
48	6927	33.8	7	263	0.42	2.23	Darfield, New Zealand	2010	LINC
49	6962	26.9	7	296	0.45	3.03	Darfield, New Zealand	2010	ROLC

2.2 *Element tests*

In order to calculate the CSR_{15} and CSR_{20} of the sand (i.e, the cyclic stress ratio that the sand can sustain until it liquefies with 15 and 20 cycles of constant stress amplitude), direct simple shear tests (element tests) were simulated in FLAC® assuming the conditions of the middle sand layer used in the column model. This means that for each soil profile of the column model, 10 element tests were performed just varying the peak cyclic stress ratio (0.600, 0.500, 0.400, 0.300, 0.260, 0.220, 0.180, 0.140, 0.10, 0.060).

Liquefaction was assumed to occur at a pore pressure ratio ($ru=\Delta u/\sigma'_{v0}$) of 0.9. Counting the number of cycles up to liquefaction for all element tests of a certain sand (corresponding to one soil profile), a graph like Figure 1 allows the identification of CSR_{15} and CSR_{20}. If the number of cycles to liquefy a soil are all lower than 20 (or 15) the minimum CSR is taken, while if they are higher than 20 (or 15) the maximum is used.

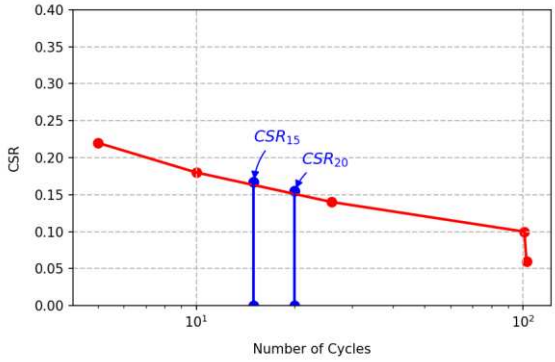

Figure 1. Identification of CSR_{15} and CSR_{20} for the sand layer of each soil profile.

3 COMPARISON BETWEEN SBM, EBM, AND NUMERICAL ANALYSIS

Before presenting the comparison of the methods it should be noted that the relationship used by Kokusho (2013) between the CSR_{20} and the N_{SPT} is the one proposed in the Japan Road Association (2002) and it is not the same as the relation proposed by Idriss & Boulanger (2010) which uses the CSR_{15}. On the other hand, the relationships proposed by Kokusho (2013) between the dissipated energy and CSR_{20} for 5% and 2% of double amplitude axial strain (DA) are shown in Figure 2 together with the FLAC® data. The proposed equation for DA = 2% agrees well with the FLAC® data which used a relatively low liquefaction threshold of ru=0.9. Since the relationship between ru and normalised dissipated energy follows aproximately an hyperbolic or power trend (e.g., Jafarian, Towhata, et al., 2012), a small change in ru threshold (eg., 0.9 to 0.95) has a significant effect of the normalised dissipated energy variation. This poses a potentially major drawback of the EBM as different ru thresholds require very different dissipated energy values. Since the CSR_{20} or CSR_{15} values do not change much when the liquefaction criterion changes it was considered a good parameter to establish the comparison between the methods. So, the CSR_{15} and CSR_{20} taken from the elements tests were used as the starting point to implement the SBM and EBM, respectively.

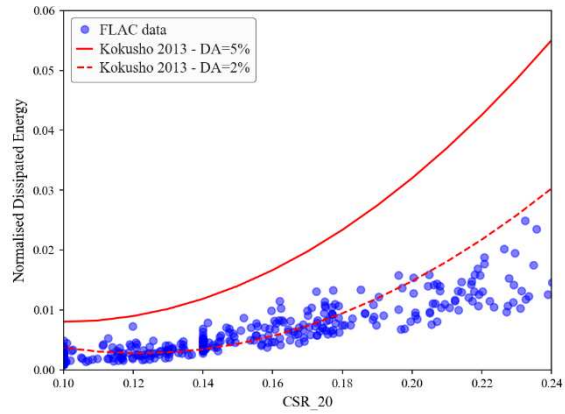

Figure 2. Relationship between normalised dissipated energy and CSR_{20}

To analyse whether the SBM and EBM made good liquefaction predictions, the number of occurences of liquefied and non liquefied cases in FLAC® were compared to number of occurences where the EBM or SBM did not predicted well.

These histograms for the different PGA values are presented in Figure 3 and 4 for the SBM and EBM respectively.

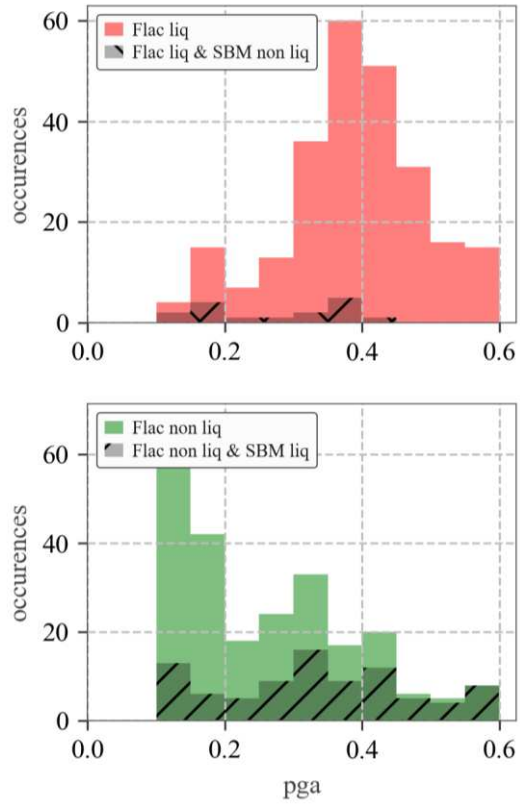

Figure 3. Histograms comparing the predictions obtained in the SBM in relation to the numerical analysis from FLAC®.

For the implementation of the EBM from Kokusho (2013) the upward energy was calculated using the upward energy at the base of the soil profile (Equation 4) which was then converted to the energy at the layer depth by the impedance ratio (β), as Equation 5:

$$E_u = \rho V_S \int (\ddot{u})^2 \, dt \quad (4)$$

where,

$\ddot{u}$ is the particle velocity of seismic waves propagating in the upward direction; ρ is the soil density; Vs is the S-wave velocity.

$$\beta = \frac{E_{u,i}}{E_{u,base}} = \left(\frac{(\rho V_S)_i}{(\rho V_S)_{base}}\right)^{0.7} = \alpha^{0.7} \quad \alpha < 1 \quad (5)$$

For the present study only the middle point of the second layer was analysed in both SBM and EBM. For that reason, no cumulative sum was used in the EBM assuming a virtual layer of 1 m thickness around that point. It should be noted that since the layer thickness only appears on the capacity side of EBM, the choice of layer thickness heavily impacts the calculation of the factor of safety (Seculin, 2018). So, to be consistent with the majority of works by Kokusho (2013) at thickness of 1 m was chosen.

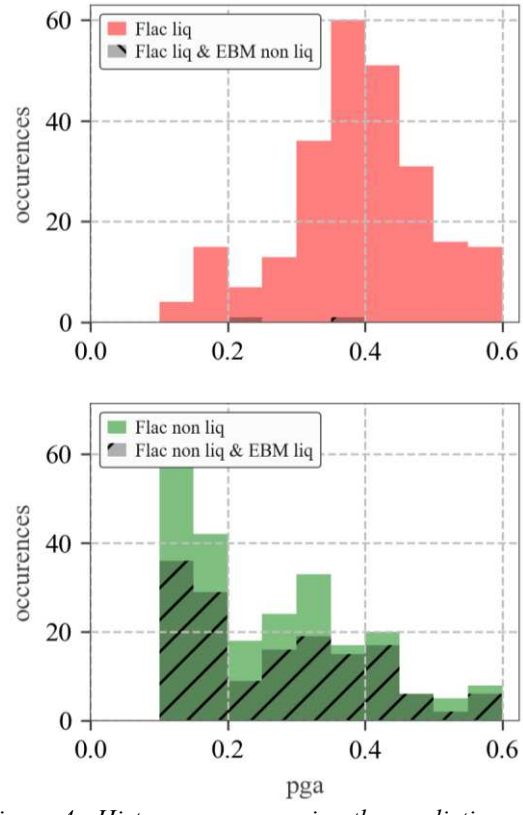

Figure 4. Histograms comparing the predictions obtained in the EBM in relation to the numerical analysis from FLAC®.

From Figures 3 and 4 it is clear that in the liquefied cases there is a much better agreement than in the non liquefied cases. The SBM seems to have slightly better results in comparison with the EBM especially for low PGA values. In fact, both methods have worst results for higher PGA values. In Figures 5 and 6 the same histograms

are presented for different relative density (D_r) values of the liquefiable layer. In most cases, liquefaction tends to be overpredicted by the EBM and SBM methods in comparison with the FLAC® results.

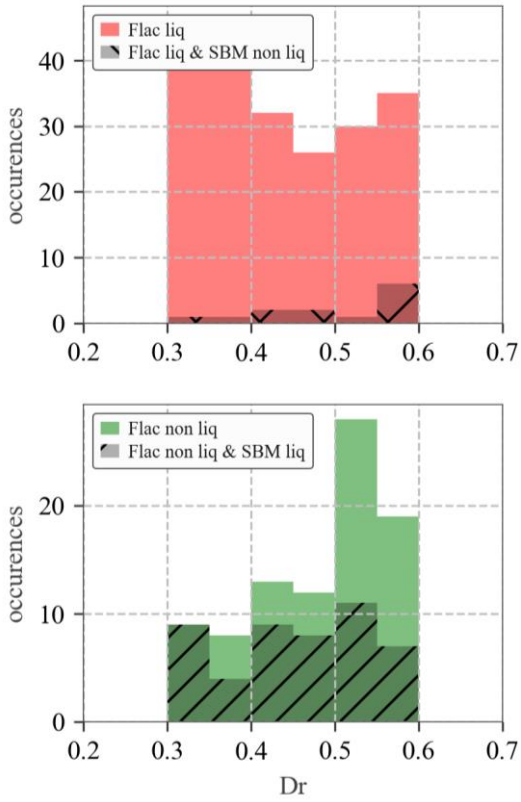

Figure 5. Histograms comparing the predictions obtained in the SBM in relation to the numerical analysis from FLAC®.

4 CONCLUSIONS

In this work a comparison was made between 500 numerical analysis performed in FLAC® and two different simplified methods presented by Boulanger and Idriss (2016) and Kokusho (2013). The results show that the simplified methods tend to overpredict liquefaction in the cases where the sand did not liquefy in the numerical analysis. These analysis were made for different PGA values and relative densities of the liquefiable layer. This overprediction tends to be more significant for higher PGA values.

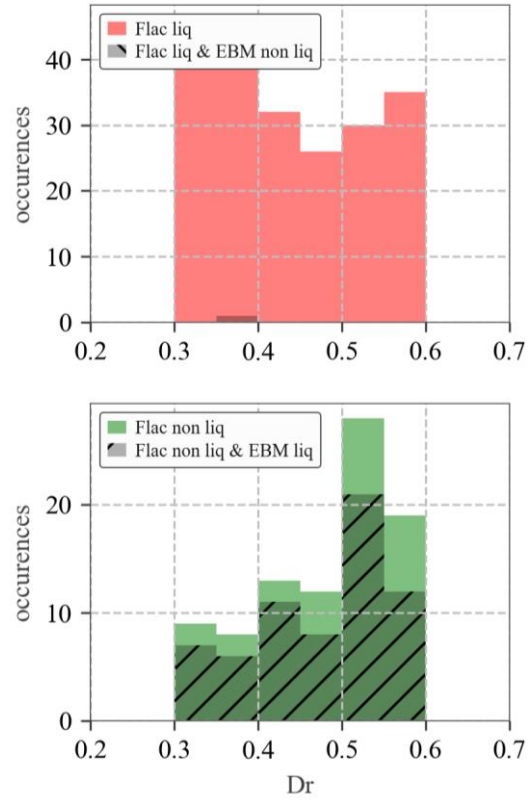

Figure 6. Histograms comparing the predictions obtained in the EBM in relation to the numerical analysis from FLAC®.

5 ACKNOWLEDGEMENTS

LIQUEFACT project (www.liquefact.eu) has received funding from the European Union's Horizon 2020 research and innovation programme under grant agreement GAP-700748. This work was financially supported by: UID/ECI/04708/2019- CONSTRUCT - Instituto de I&D em Estruturas e Construções funded by national funds through the FCT/MCTES (PIDDAC).The authors also acknowledge the Portuguese Foundation for Science and Technology (FCT) on scholarship SFRH/BPD/85863/2012.

6 REFERENCES

Ancheta, T. D., Darragh, R. B., Stewart, J. P., Seyhan, E., Silva, W. J., Chiou, B. S.-J., … Donahue, J. L. (2013). PEER NGA-West2 Database PEER Report No. 2013/03. *Pacific Earthquake Engineering Research Center, University of California, Berkeley*, *03*, 134.

Boulanger, R. W., & Idriss, I. M. (2016). CPT-Based Liquefaction Triggering Procedure. *J. of Geotechnical and Geoenvironmental Engineering*, *142*(2), 04015065. https://doi.org/10.1061/(ASCE)GT.1943-5606.0001388

Boulanger, R., & Ziotopoulou, K. (2015). A sand plasticity model for earthquake engineering applications, *UCD/CGM-15*(May), 1–114. https://doi.org/10.1016/j.soildyn.2013.07.006

Bray, J. D., Markham, C. S., & Cubrinovski, M. (2017). Liquefaction assessments at shallow foundation building sites in the Central Business District of Christchurch, New Zealand. *Soil Dynamics and Earthquake Engineering*, *92*(10), 153–164. https://doi.org/10.1016/j.soildyn.2016.09.049

Chiaradonna, A., Tropeano, G., d'Onofrio, A., & Silvestri, F. (2018). Development of a simplified model for pore water pressure build-up induced by cyclic loading. *Bulletin of Earthquake Engineering*, *16*(9), 3627–3652. https://doi.org/10.1007/s10518-018-0354-4

Davis, R., & Berril, J. (1982). Energy dissipation and seismic liquefaction in sands. *Earthquake Engineering & Structural Dynamics*, *10*(1), 59–68. https://doi.org/10.1002/eqe.4290100105

Dobry, R., Pierce, W., Dyvik, R., Thomas, G., & Ladd, R. (1985). Pore pressure model for cyclic straining of sand. *Civil Engineering Department, Rensselaer Polytechnic Insti-Tute, Troy*.

Finn, W., & Bhatia, S. (1982). Prediction of seismic porewater pressures. In *Proceedings of the 10th international conference on soil mechanics and foundation engineering* (pp. 201–206).

Idriss, I., & Boulanger, R. W. (2010). SPT-based liquefaction triggering procedures, (December). https://doi.org/UCD/CGM-10/02

Ivšić, T. (2006). A model for presentation of seismic pore water pressures. *Soil Dynamics and Earthquake Engineering*, *26*(2–4), 191–199. https://doi.org/10.1016/j.soildyn.2004.11.025

Jafarian, Y., Towhata, I., Baziar, M. H., Noorzad, A., & Bahmanpour, A. (2012). Strain energy based evaluation of liquefaction and residual pore water pressure in sands using cyclic torsional shear experiments. *Soil Dynamics and Earthquake Engineering*, *35*, 13–28. https://doi.org/10.1016/j.soildyn.2011.11.006

Japan Road Association. (2002). *Liquefaction potential evaluation method. Design code for bridges; seismic design.*

Kokusho, T. (2013). Liquefaction potential evaluations: energy-based method versus stress-based method. *Canadian Geotechnical J.*, *50*(10), 1088–1099. https://doi.org/10.1139/cgj-2012-0456

Nemat-Nasser, S., & Shokooh, A. (1979). A unified approach to densification and liquefaction of cohesionless sand in cyclic shearing. *Canadian Geotechnical J.*, *16*(4), 659–678. https://doi.org/10.1139/t79-076

Park, T., Park, D., & Ahn, J. K. (2015). Pore pressure model based on accumulated stress. *Bulletin of Earthquake Engineering*, *13*(7), 1913–1926. https://doi.org/10.1007/s10518-014-9702-1

Seed, H. ., Idriss, I., Makdidi, F., & Nanerjee, N. (1975). Representation of irregular stress time histories by equivalent uniform stress series in liquefaction analyses Report No. EERC 75–29. *Earthquake Engineering Research Center, Univ California Berkeley*.

Seculin, D. (2018). *Energy-based versus stress-based liquefaction triggering assessment*. MSc Thesis submitted to the Technical University of Civil Engineering in Bucharest, Romania